



Study of the Nuclear Structure Properties in Strontium ($^{90,92,94}\text{Sr}$) Isotopes Using Nuclear Shell-model Calculations

Fatema Hameed Obeed and Ali Khalaf Hasan

Department of Physics, Faculty of Education for Girls, University of Kufa, Najaf, Iraq



LINK	RECEIVED	ACCEPTED	PUBLISHED ONLINE	ASSIGNED TO AN ISSUE
https://doi.org/10.37575/b/sci/240008	03/02/2024	14/07/2024	14/07/2024	01/12/2024
NO. OF WORDS	NO. OF PAGES	YEAR	VOLUME	ISSUE
3936	5	2024	25	2

ABSTRACT

In the current research, various nuclear properties energy spectrum, reduced electromagnetic transition probabilities, nuclear moments, and the distributions of both the nuclear charge and mass density as a function of radial distance from the nucleus center (r) were computed for $^{90,92,94}\text{Sr}$ isotopes' using the NuShellX@MSU code. The Skyrme (SLy4) potential was utilized to compute the Strontium isotopes' wave functions with mass numbers 90, 92, and 94. By employing the Gloeckner interaction and bare G-matrix, the computed results showed good agreement with the available experimental information on the aforementioned nuclear features of all the above isotopes. Additionally, the spins and parities of energy levels were confirmed and determined in accordance with certain empirical values. Furthermore an acceptable agreement for transition strengths $B(E2; 2_1^+ \rightarrow 0_1^+)$ for $^{90,92,94}\text{Sr}$, and the dipole magnetic moment of the ground state in the ^{90}Sr isotope, was observed with the available experimental values. In these calculations, new values were predicted for the above nuclear properties, which had not been previously determined experimentally.

KEYWORDS:

energy spectra; gloeckner interaction; model space; nuShellX code; skyrme potential; transition strengths

CITATION

Obeed, F.H. and Hasan, A.K. (2024). Study of the nuclear structure properties in strontium ($^{90,92,94}\text{sr}$) isotopes using nuclear shell-model calculations. *Scientific Journal of King Faisal University: Basic and Applied Sciences*, 25(2), 1–5. DOI:10.37575/b/sci/240008

1. Introduction

Nuclear shell-model calculations are essential for the theoretical framework used by both experimentalists and theoreticians to explain many nuclear structure properties (Salman and Hameed, 2022; Hasan *et al.*, 2021). This microscopic model of the atomic nucleus is one of the most fundamental nuclear models, presuming that nucleons occupy discrete energy levels and have specified angular momentum. In the ground state, an isotope's nucleons will be in the lowest possible energy state (Lawson, 1980). Isotopes in the mass region greater than or equal to 90 provide a rare opportunity to examine the effects of the proton subshell closure at 38 and the neutron shell closure at 50 on level arrangements. A substantial number of studies have recognized that the nuclear level arrangements in the mass region greater than or equal to 90 can be well defined within the shell-model framework. For instance, many nuclear properties of certain nuclei have been well identified within this framework. Heng *et al.* studied the level structure of the ^{90}Nb isotope using the NuShellX code (Heng *et al.*, 2019). N. S. Pattabiraman *et al.*, (2002) discussed the level structure of ^{92}Mo , considering proton subshell closure at 38 and neutron shell closure at 50. In their study, the configuration space included four proton orbits (from $f_{5/2}$ to $g_{9/2}$) and six neutron orbits (from $p_{1/2}$ to $s_{1/2}$). Rainovski *et al.*, (2002) described the high-spin levels of the ^{90}Y nucleus, with computations carried out in the proton orbits ($0f_{5/2}$ to $0g_{9/2}$) and neutron orbits ($1p_{1/2}, 0g_{9/2}, 1d_{5/2}$), including an extended configuration with neutrons in the $0g_{7/2}$ orbital using Ritschil code. The high levels of these isotopes arose from the configurations of a single $g_{9/2}$ neutron into the $d_{5/2}$ level through the neutron shell closure at 50. In particular, isotones with proton numbers equal to 38 in the mass number region of 90, 92, and 94 have been significant topics for examining the lasting interactions in shellmodel calculations and two-particle excitations.

The isotopes $^{90,92,94}\text{Sr}$ appear to be perfect candidates for such a study to better interpret the nuclear features of isotopes in the mass region

greater than or equal to 90.

This research aims to perform shellmodel calculations using the NuShellX@MSU code to describe several nuclear properties of the $^{90,94,94}\text{Sr}$ isotopes.

2. Theory

Studying the transition probabilities $B(E2)$ can provide new and important information about the development of nuclear properties and the shell-model. The electromagnetic transition from an initial nuclear level (i), where the nucleus can be at rest, to a final nuclear level (f), results in the nucleus's momentum in state (f) and the emitted gamma ray being identical. The electromagnetic transition between them can only occur when the emitted photon carries away an amount of angular momentum (ℓ) such that $J_f = J_i + \ell$ (Brown, 2005):

$$|J_i - J_f| \leq \ell \leq J_i + J_f, (1)$$

Where ($J = |J|$).

The gamma transition rate is specified by E , the multipolarity (ΔE), the transition energy, and a factor that depends upon the details of the internal nuclear structure (Preetha and Kumar, 2017). The electromagnetic transition probabilities of $B(E2)$ and $B(M1)$ of the transition between initial and final states J_i and J_f may be given according to the following formula (Aghahasani *et al.*, 2022; Obeed, 2021):

$$B(E2; J_i \rightarrow J_f) = \frac{e^2}{(2J_i+1)} | \langle J_f M_f | \hat{Q}_2 | J_i M_i \rangle |^2, (2)$$

$$B(M1; J_i \rightarrow J_f) = \frac{\mu_N^2}{(2J_i+1)} | \langle J_f M_f | \hat{M}_1 | J_i M_i \rangle |^2, (3)$$

where \hat{Q}_2 and \hat{M}_1 are operators of the nuclear moments.

Electric quadrupole moments are another essential quantity to characterize the nuclei's shapes, which are linked to the intrinsic quadrupole moments by the following relationship (Obeed, 2021):

$$Q_s(JK) = \frac{3K^2 - J(J+1)}{(2J+3)(J+1)} Q_0, \quad (4)$$

where K represents the total angular momentum projection on the nuclear symmetry axis, J is the spin, and Q_0 is the intrinsic quadrupole moment.

Intrinsic quadrupole moments are defined according to the following relationship (Obeed and Hasan, 2021):

$$Q_0 = \sqrt{\frac{16\pi}{5e^2}} \cdot (B(E2))^{1/2}, \quad (5)$$

where $Q_s > 0$ indicates the prolate deformation shape of nuclei, $Q_s < 0$ designates the oblate deformation shape of the isotopes, and $Q_s = 0$ indicates the spherical shape. The magnetic moments are given by the following formula (Carchidi *et al.*, 1986):

$$\mu(J=1) = \begin{bmatrix} J & 1 & J \\ -J & 0 & J \end{bmatrix} \times \frac{\sqrt{4\pi}}{3} \langle J || \hat{O}(M1) || J \rangle \mu_N, \quad (6)$$

where $\langle J || \hat{O}(M1) || J \rangle \mu_N$ represents the operator of the magnetic transition, $\mu_N = \frac{e\hbar}{2m_p c} = 0.1051 \text{ e.f.m}$, μ_N is the nuclear magnetons, and m_p is the proton mass.

Here, $\begin{bmatrix} J & 1 & J \\ -J & 0 & J \end{bmatrix}$ represents the $3j$ symbol for the angular momentum factor, the value of which is given by (Carchidi *et al.*, 1986):

$$\begin{bmatrix} J & 1 & J \\ -J & 0 & J \end{bmatrix} = \left[\frac{J(2J-1)}{(2J+1)(J+1)(2J+3)} \right]^{0.5}, \quad (7)$$

The calculations in Eq. (6) require knowing the values of the magnetic moments (g) factors: $g_p^p = 1$, $g_s^p = 5.585$ for protons and $g_n^p = 0$, $g_s^n = -3.826$ for neutrons (Heyde and Irvine, 1990).

In the calculations, the density distribution of a system containing A nucleons was calculated and given according to the following relationship (Roy and Nigam, 1967):

$$\rho_0(r) = \sum_{i=1}^A |\varphi_i(\vec{r})|^2, \quad (8)$$

3. Results and Discussion

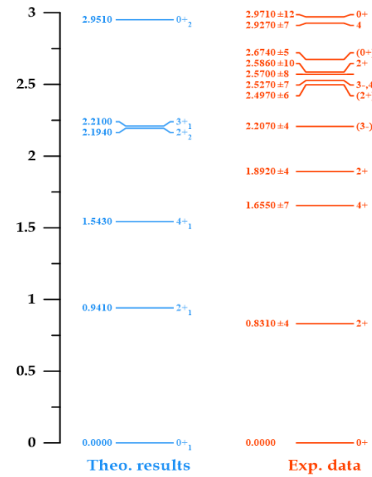
In this research, various nuclear characteristics of strontium isotopes ($^{90,92,94}\text{Sr}$) with neutrons ($N = 52, 54$ and 56) were calculated using the NuShellX@MSU code, which is a shell model code written by Bill Rae. This code can be used to determine the particular energies and eigenvectors of low states in shell-model Hamiltonian matrix computations, as well as the magnitude and beta decay, and radial wave functions were computed using Skyrme capabilities (Sly4) from the same code (Brown and Rae, 2014) with energetic charge nucleons and factor (g). The Gloeckner space model for the orbitals of the proton ($2p_{1/2}$, $1g_{9/2}$) and neutron ($3s_{1/2}$, $2d_{5/2}$) with the Gloeckner interaction and bare G -matrix was performed for the valence particles (two neutrons, four neutrons, and six neutrons) of the isotopes ^{90}Sr , ^{92}Sr , and ^{94}Sr , respectively, outside ^{88}Sr , which is a closed core. Single-particle energies of a valence nucleon are represented by the values $\varepsilon_{2p_{1/2}}(p) = -7.124 \text{ MeV}$, $\varepsilon_{1g_{9/2}}(p) = -6.248$, $\varepsilon_{3s_{1/2}}(n) = -5.506 \text{ MeV}$ and $\varepsilon_{2d_{5/2}}(n) = -6.338 \text{ MeV}$. The calculations and results of each isotope are discussed in the following sections.

3.1. Energy levels:

The ^{90}Sr isotope: This isotope has two neutrons scattered in orbitals ($3s_{1/2}$, $2d_{5/2}$) over the ^{88}Sr closed core. Figure 1 presents theoretical and experimental excitation spectra values for the ^{90}Sr isotope. An

agreement was achieved for the ground state (0_1^+) of the calculated energy level, which was compared to the experimental energy level in the same ground state (0_1^+). An acceptable agreement was also found for theoretical energies values $\{0.941, 1.543, 2.194, \text{ and } 2.951\} \text{ MeV}$ associated with the states (total angular momentum and parity) $\{2_1^+, 4_1^+, 2_2^+, \text{ and } 0_2^+\}$, which were compared with the values of the experimental energies $\{0.831_{-4}^+, 1.655_{-7}^+, 1.892_{-4}^+, \text{ and } 2.971_{-12}^+\} \text{ MeV}$ (Basu and McCutchan, 2020). Current calculations have suggested that the state associated with (3^-) with the experimental energy value 2.207_{-4}^+ MeV can be confirmed by the calculated theoretical state (3_1^+); this is due to the accepted agreement of the above energy value with the theoretical energy value of 2.210 MeV . It was noted that there are values of energies and their accompanying states $\{ \text{from } 2.497_{\pm 6}; (2^+) \text{ to } 2.927_{\pm 7}; 4\}$ MeV in the experimental data for which no corresponding values appeared in the calculations. The highest theoretical value for the energy 2.951 MeV in the state 0_2^+ was obtained, while the experimental values are higher.

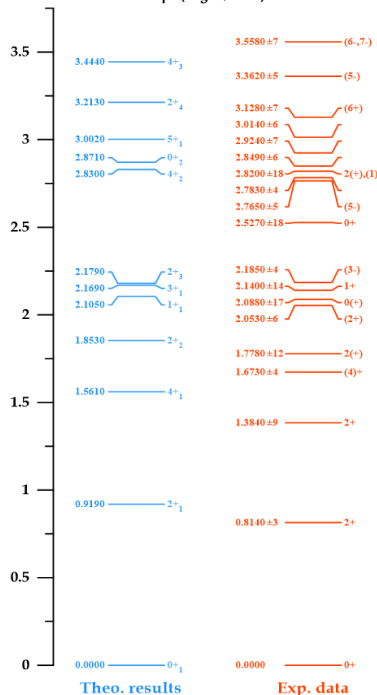
Figure 1. Comparison between the calculated level energy values and the experimental data of the ^{90}Sr isotope (Basu and McCutchan, 2020)



The ^{92}Sr isotope has four nucleons (neutrons) dispersed in orbitals $3s_{1/2}$ and $2d_{5/2}$ over the closed nucleus ^{88}Sr . Figure 2 displays the experimental and theoretical excitation spectra values for the isotope ^{92}Sr as follows (Baglin, 2012): a complete agreement was found for the ground state (0_1^+) that is compared to the ground state in experimental information. A certain extent of predictable agreement of theoretical energy values was also found (0.919 and 2.105) between the MeV of the states 2_1^+ and 1_1^+ and the experimental energy values (0.814 ± 3 and 2.140 ± 14 MeV) in the same states. Through the calculated theoretical state (3_1^+), confirmation of the state associated (3^-) with the experimental energy level (2.185 ± 4 MeV) was obtained; this is due to the acceptable agreement of this level with the theoretical level (2.169 MeV). A probable assertion of the spin only (4) at the experimental level value (1.673 ± 4 MeV) was found due to the acceptable compatibility of this energy value with the theoretical value (1.561 MeV). The parity (+) was confirmed for the experimental energy value 1.778 ± 12 MeV associated with the spin (4), and the states (4_2^+ , 0_2^+ , 5_1^+ and 2_1^-) were identified. In terms of the experimental energy values (2.783 ± 4, 2.849 ± 6, 2.924 ± 7, and 3.014 ± 6) these energies were compatible to an acceptable extent with the theoretical energy's values of 2.830, 2.871, 3.002, and 3.213 MeV. New theoretical energy levels (2.179 and 3.444 MeV) of the states 2_3^+ and 4_3^+ were predicted in these calculations but still have no experimental energy value for comparison with. There are empirical energy values that have recently been observed: (1.384 ± 9, 2^+), (2.053 ± 6, 2^+), (2.088 ± 17, 0^+), (2.527 ± 4, 0^+), (2.765 ± 5, 5^-),

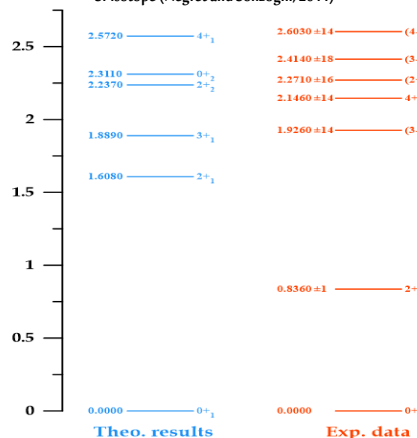
($2.783_{-4}^{+4}, \dots$), ($2.820_{-18}^{+18}, 2^+(1)$), ($3.128_{-7}^{+7}, (6^+)$), and ($3.558_{-7}^{+7}, (6^-, 7^-)$) which have no assessment with theoretical energies values. Through the current study, it was observed that the highest value of the theoretical energy was 3.444 MeV with the state 4_{-3}^+ , while higher values have been observed experimentally.

Figure 2. Comparison between the calculated level energy values and the experimental data of the ^{92}Sr isotope (Baglin, 2012)



The ^{94}Sr isotope: This isotope has six nucleons (neutrons) dispersed in the orbits $3s_{1/2}, 2d_{5/2}$ over the ^{88}Sr closed core. Figure 3 presents the theoretical and experimental excitation spectra values for the ^{94}Sr isotope (Negret and Sonzogni, 2011). Here, theoretically, the calculated energy level and its ground state (0^+) were in complete agreement with the experimental ground state (0^+), and there was a predictable confirmation of the states (3^-), (2^+), and (4^-) for experimental energy levels ($1.926_{-14}^{+14}, 2.271_{-16}^{+16}$ and $2.603_{-14}^{+14} \text{ MeV}$). There was a largely appropriate agreement between these energies and the theoretical energies values ($1.889, 2.237$ and 2.572 MeV). There are empirical energy values with the state ($2.146_{-14}^{+14}, 4^+$, and $2.414_{-18}^{+18}, (3^-)$ MeV) that have recently been observed and have no corresponding theoretical values.

Figure 3. Comparative between the calculated level energy values and the experimental data of the ^{94}Sr isotope (Negret and Sonzogni, 2011)



3.2. Electromagnetic transition probabilities $B(E2)$, $B(M1)$:

The results of electric quadrupole transition probabilities were calculated by selecting the effective nucleon charges of protons and neutrons as follows: ($e_p=1.830e, e_n=1.66e$), ($e_p=1.772e, e_n=1.544e$), and ($e_p=1.655e, e_n=1.31e$), while the parameter values meters of the orbital and spin nucleon (g) factors $g_s(p)$, $g_s(n)$, $g_l(p)$ and $g_l(n)$ were equal to ($5.027, -3.443, 1.671, 0.671$), ($5.027, -3.443, 1.02, 0.02$), and ($5.027, -3.443, 1.0$), which, in turn, were used to correspondingly calculate the dipole magnetic $B(M1)$ for $^{90,92,94}\text{Sr}$ isotopes. The calculated values of reduced electromagnetic transition possibilities are listed in Tables 1, 2, and 3 for $^{90,92,94}\text{Sr}$ isotopes. These tables display the $E2$ and $M1$ transition for the ^{90}Sr isotope. The computed $B(E2)$ transition possibilities were in good agreement with the experimental data (Basu and McCutchan, 2020), specifically for the strong ($E2$) decays from 2_1^+ state to 0_1^+ state the value $B(E2; 2_1^+ \rightarrow 0_1^+) = 203.6 \pm_{19}^{33} e^2 fm^4$, which perfectly agreed with the experimental data ($E2; 2_1^+ \rightarrow 0_1^+) = 204.2 e^2 fm^4$. The calculated value for the $E2$ and $M1$ transition strength values $B(E2; 3_1^+ \rightarrow 2_1^+) = 32.3 e^2 fm^4$ and $6.163 \times 10^{-2} \mu_N^2$ with transition strengths of $B(E2; 3_1^+ \rightarrow 4_1^+) = 306.9 e^2 fm^4$ were not clearly categorized in the experimental data ($E1, M2, E1$) for the corresponding values.

In these calculations, the transition strength was predicted for $E2, M1$, and $E2$. The transition strengths $E2$ and $M1$ for the ^{92}Sr isotope are listed in Table 2. This comparison displays that the calculated values in this study of the transition possibilities agreed with the empirical formation (Baglin, 2012), especially the ($E2$) transition strengths $B(E2; 2_1^+ \rightarrow 0_1^+) = 197.6 e^2 fm^4$ with the experimental value $197.3 \pm_{3}^{3} e^2 fm^4$. In the calculations for $E2$ and $M1$ transition strengths of $1_1^+ \rightarrow 2_1^+$ of the values $302.4 e^2 fm^4$ and $5.13 \times 10^{-2} \mu_N^2$ were found in comparison to the experimental values of $0.740 \pm_{16} e^2 fm^4$ and $0.125 \times 10^{-2} \pm_{3} \mu_N^2$ respectively. Lastly, Table 3 presents the comparison of the experimental (Negret and Sonzogni, 2011) and calculated ($E2$ and $M1$) transition strength values for the ^{94}Sr isotope. These comparisons clarified that the foretold $E2$ transition strength from $2_1^+ \rightarrow 0_1^+$; $203.8 e^2 fm^4$ well agreed with the experimental value $203.1 \pm_{4} e^2 fm^4$. $E2$ values and $M1$ transition strengths were calculated for the transitions ($3_1^+ \rightarrow 2_1^+$ and $4_1^+ \rightarrow 3_1^+$) that created the values $9.498 \times 10^{12} e^2 fm^4$, $0.521 \mu_N^2$, and $49.3 e^2 fm^4$. These values were unverified in multi-polarity ($E1$ and $E1+M2$) in experimental data, but recent calculations have predicted $E2, M1$, and $E2$ transition strengths. A new electromagnetic transition of several $B(E2; \downarrow)$ and $B(M1; \downarrow)$ of $^{90,92,94}\text{Sr}$ isotopes was observed (as shown in Tables 1, 2, and 3), where there were no observations in the experimental data. More information on the theoretical knowledge of all isotopes regarding energy levels and electromagnetic transitions will be added.

Table 1. Theoretical comparison between the values of the electromagnetic transition probabilities for positive-parity spin states in the ^{90}Sr isotope and empirical values (Basu and McCutchan, 2020).

$J_i \rightarrow J_f$	Theoretical Results			Experimental Results	
	$(BE2 \downarrow) (e^2 fm^4)$	$(BM1 \downarrow) (\mu_N^2)$	multi-polarity	$(BE2 \downarrow) (e^2 fm^4)$	$(BM1 \downarrow) (\mu_N^2)$
$2_1^+ \rightarrow 0_1^+$	204.2	-----	E2	$203.6 \pm_{19}^{33}$	-----
$4_1^+ \rightarrow 2_1^+$	159.3	-----	E2	$124.5 \pm_{11}^{11}$	-----
$3_1^+ \rightarrow 2_1^+$	32.36	6.163×10^{-2}	(E1, M2)	$> 2.87 \times 10^{-3}$	-----
$3_1^+ \rightarrow 4_1^+$	306.9	-----	(E1)	$> 198.8 \times 10^5$	-----

Table 2. Theoretical comparison between the electromagnetic transition probabilities for positive-parity spin states in the ^{92}Sr isotope and experimental data (Baglin, 2012)

$J_i \rightarrow J_f$	Theoretical Results			Experimental Results	
	$(BE2 \downarrow) (e^2 fm^4)$	$(BM1 \downarrow) (\mu_N^2)$	multi-polarity	$(BE2 \downarrow) (e^2 fm^4)$	$(BM1 \downarrow) (\mu_N^2)$
$2_1^+ \rightarrow 0_1^+$	197.6	-----	E2	$197.3 \pm_{3}^{3}$	-----
$4_1^+ \rightarrow 2_1^+$	57.51	-----	E2	-----	-----
$1_1^+ \rightarrow 2_1^+$	302.4	5.13×10^{-2}	E2+M1	$0.740 \pm_{16}^{16}$	$0.125 \times 10^{-2} \pm_{3}^{3}$
$3_1^+ \rightarrow 2_1^+$	37.72	3.49×10^{-2}	-----	-----	-----
$3_1^+ \rightarrow 4_1^+$	40.56	-----	-----	-----	-----
$3_1^+ \rightarrow 1_1^+$	41.04	-----	-----	-----	-----
$5_1^+ \rightarrow 4_1^+$	156.3	0.1584×10^{-2}	-----	-----	-----
$5_1^+ \rightarrow 3_1^+$	129.3	-----	-----	-----	-----

Table 3. Theoretical comparison between the electromagnetic transition probabilities for positive-parity spin states in the ^{90}Sr isotope and experimental data (Negret and Sonzogni, 2011)

$J_i \rightarrow J_f$	Theoretical Results		Experimental Results	
	(BE2 ↓)($e^2\text{fm}^4$)	(BM1 ↓)(μ_N^2)	multi-polarity	(BE2 ↓)($e^2\text{fm}^4$)
$2_1^+ \rightarrow 0_1^+$	203.8	-----	E2	$203.1 \pm \frac{1}{4}$
$3_1^+ \rightarrow 2_1^+$	9.498×10^{-2}	0.5212	(E1)	-----
$4_1^+ \rightarrow 2_1^+$	137.5	-----	E2	-----
$4_1^+ \rightarrow 3_1^+$	149.3	-----	(M1+E2)	-----

3.3. Electric quadrupole and magnetic dipole moments:

Nuclear shape is a fundamental property of the nucleus that describes nuclear structure and many nuclear properties. The current research contains the nuclear moments (Q_s) and (μ) of $^{90,92,94}\text{Sr}$ isotopes, which were calculated and are shown in Table 4. The electric quadrupole moment was calculated for all isotopes using shell-model calculations, but there are, yet no observations in the experimental data. Through these calculations, it was observed that the quadrupole electrical moment of the ^{90}Sr isotope at the 2_1^+ , 4_1^+ , and 3_1^+ states, as well as the states 2_1^+ , 3_1^+ , and 5_1^+ in the ^{92}Sr isotope exhibited negative signs representing the dominance of the oblate shape. Moreover, the state 4_1^+ in the ^{92}Sr isotope and the 2_1^+ , 4_1^+ , and 3_1^+ states of the ^{94}Sr isotope appeared with positive marks representing the prolate shape dominance of these states. Table 4 shows the calculated results of dipole magnetic (μ) moments of the ^{90}Sr isotope. This indicated that the 2_1^+ and 4_1^+ states had values of $0.241\mu_N$ and $-0.608\mu_N$, which were predicted in reasonable agreement with the experimental data (Basu and McCutchan, 2020): $-0.24 \pm \frac{22}{22}\mu_N$ and $-0.08 \pm \frac{68}{68}\mu_N$ of the 2_1^+ and 4_1^+ states, respectively. In this study, the calculations yielded many values of dipole magnetic (μ) moments of $^{90,92,94}\text{Sr}$ isotopes, such as (3_1^+ , -2.102) μ_N for the ^{90}Sr isotope (2_1^+ , -1.365), (4_1^+ , -2.689), (3_1^+ , -3.403), (1_1^+ , -0.02) and (5_1^+ , 4.749) (μ_N) for the ^{92}Sr isotope. Finally, 2_1^+ , 3_1^+ , and 4_1^+ for the ^{94}Sr isotope were underestimated empirically, with values of -0.743 , -3.443 , and -2.754 , respectively.

Table 4. Theoretical comparison between the values of the nuclear moments in $^{90,92,94}\text{Sr}$ isotopes and empirical data using G1 model space.

Isotopes	Theoretical Results			Experimental Results	
	J_i^π	(Q) (efm ²) Sky29	μ (μ_N)	(Q) (efm ²)	μ (μ_N)
^{90}Sr	2_1^+	-0.35	-0.241	-----	$-0.24 \pm \frac{22}{22}$
	4_1^+	-21.05	-0.608	-----	$-0.08 \pm \frac{68}{68}$
	3_1^+	-26.31	-2.102	-----	(Basu and McCutchan, 2020)
^{92}Sr	2_1^+	-24.15	-1.365	-----	-----
	4_1^+	18.75	-2.689	-----	-----
	3_1^+	-1.57	-3.403	-----	-----
	1_1^+	0	0.02	-----	-----
	5_1^+	-4.37	-4.749	-----	-----
^{94}Sr	2_1^+	28.81	-0.743	-----	-----
	3_1^+	20.86	-3.443	-----	-----
	4_1^+	16.68	-2.754	-----	-----

$Q_1=2_1^+, 4_1^+, 3_1^+, 5_1^+$

3.4. Density distributions of charge and mass in nuclei:

The nuclear charge and mass density distributions of $^{90,92,94}\text{Sr}$ isotopes were calculated and are shown in Figures 4, 5, and 6, respectively. These figures illustrate charge density distribution values of $^{90,92,94}\text{Sr}$ isotopes, which were centered at the nucleus midpoint with values of $\rho_{ch} = \{0.07981, 0.08165, \text{ and } 0.08358\}$ Ze/fm^3 remaining stable at the specified distance $r=0.1\text{fm}$. These values for $^{90,92,94}\text{Sr}$ isotopes continued to decrease until they stabilized at zero at a distance $r=7.9\text{fm}$. The mass density distribution in $^{90,92,94}\text{Sr}$ isotopes were in the nuclei midpoint at the value $\rho_m = \{0.1614, 0.1642, \text{ and } 0.1670\}$ $\text{nuclei}/\text{fm}^3$. These values remained stable at $r = 0.1\text{fm}$. However, at a distance of $r = 0.2\text{fm}$, these values increased to $0.1617, 0.1645, \text{ and } 0.1673$ $\text{nuclei}/\text{fm}^3$. These values continued to progressively increase up to the radial distance

$=1.3, 1.4, \text{ and } 1.5\text{ fm}$ at the values $0.1684, 0.1718, \text{ and } 0.1752$ $\text{nuclei}/\text{fm}^3$ for $^{90,92,94}\text{Sr}$ isotopes, respectively. Subsequently, the mass density distributions of the studied isotopes started to decrease at distances of $1.4, 1.5, \text{ and } 1.6\text{ fm}$, reaching values of $0.1683, 0.1716, \text{ and } 0.1750$ $\text{nuclei}/\text{fm}^3$ for the $^{90,92,94}\text{Sr}$ isotopes. These values continued to decrease until stabilizing at zero at a radial distance of $r = 7.9\text{ fm}$ for all isotopes under observation in the current study. There is, as yet, no experimental data for the distributions of the nuclear density of charge and mass for $^{90,92,94}\text{Sr}$ isotopes for comparison with the present calculations.

Figure 4. Density distributions of nuclear charge and mass as a function of radial distance from the midpoint of the ^{90}Sr isotope

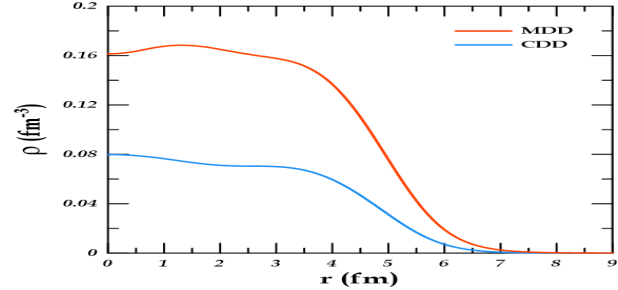


Figure 5. Density distributions of nuclear charge and mass contrary to the radial distance from the center of the ^{92}Sr isotope

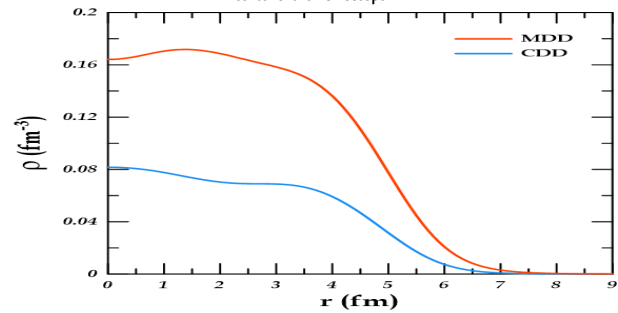
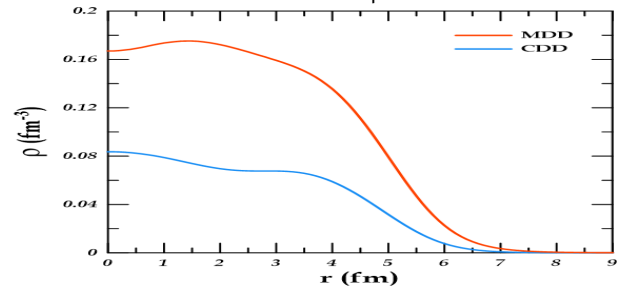


Figure 6. Density distributions of nuclear charge and mass in contrast to the radial distance from the center of the ^{94}Sr isotope



4. Conclusions

From the calculated results, the following can be concluded:

- Absolute agreement was observed between theoretical and experimental energy values, particularly for the ground state levels of $^{90,92,94}\text{Sr}$ isotopes.
- A positive parity of the ^{92}Sr isotopes was confirmed for one level of the empirical energy value.
- The states (total angular momentum and valence) of some levels in the ^{92}Sr isotope were determined for undetermined experimental energy levels.
- There was a strong agreement between the calculated quadrupole transitions and empirical data, especially evident in $B(E2; 2_1^+ \rightarrow 0_1^+)$ of the $^{90,92,94}\text{Sr}$ isotopes.
- The current calculations revealed the electric quadrupole and dipole magnetic moments. It was predicted that the ground band energy states exhibit an oblate shape for $^{90,92}\text{Sr}$ isotopes, except for one level in the ^{92}Sr isotope, which has a prolate shape. The shape of the ^{94}Sr

isotope is expected to be prolate, which led to the conclusion that the shape of some regions of the nuclear striatum is affected by structural influences and could change from one isotope to another neighbor. In addition, it was found that the shape changes with the number of neutrons and can also change with the excitation energy or state within the same nucleus. These variances occur due to the rearrangement of the structure space of the valance particles or to the dynamic response.

- Density distributions for charge and mass in the isotopes $^{90,92,94}\text{Sr}$ were identified; the density distributions were found to be in the nucleus center for (Ze/fm^{-3}) and $\rho_0(\frac{nucleon}{fm^{-3}})$ and started decreasing until fixed at zero at specific values. In contrast to the charge density distributions, the mass density distributions showed contradictory behavior, starting to increase to certain values and decreasing until they stabilized at zero at certain values of radial distance.
- The GI interaction and the GI model space were used to calculate the aforementioned nuclear properties of the $^{90,92,94}\text{Sr}$ isotopes.

Biographies

Fatema Hameed Obeed

Department of Physics, Faculty of Education for Girls, University of Kufa, Najaf, Iraq, 0096407817322815, fatimahh.alfatlawi@uokufa.edu.iq

Prof. Obeed is an Iraqi who earned her master's degree in nuclear physics from Kufa University in Iraq in 2010. She achieved the title of professor in nuclear physics in 2022. Her primary research interests include theoretical studies in nuclear physics focusing on nuclear structure using Fortran and MATLAB programming codes. She has received training in teaching methods and computer education. Dr. Obeed has actively participated in numerous local and international scientific conferences and has published ten research papers in scientific journals indexed within the Scopus platform.

ORCID: 0000-0003-2076-0376.

Ali Khalaf Hasan

Department of Physics, Faculty of Education for Girls, University of Kufa, Najaf, Iraq, 0096407802461719, alikh.alsinayyid@uokufa.edu.iq

Prof. Hasan is an Iraqi who earned his Ph.D. in nuclear physics from the University of Basra, Iraq, in 2009. His primary research interests encompass quantum, theoretical, nuclear, and radiation physics. Dr. Hasan has actively participated in numerous local scientific conferences in Iraq. He has published approximately 50 papers in scientific journals within Iraq, including 23 papers in international Scopus-indexed journals such as the International Journal of Physical Sciences, Ukrainian Journal of Physics, International Journal of Current Research, and AIP Conference Proceedings.

ORCID: 0000-0002-8126-5179

References

- Aghahasani, H., Mohammadi, S. and Sajjadi, Z. (2022). Study of high spin phenomena in even-even dysprosium isotopes by using projected shell model. *Iranian Journal of Physics Research*, **22**(3), 141–51. DOI: 10.47176/ijpr.22.3.71276
- Baglin, C.M. (2012). Nuclear data sheets for A=92. *Nuclear Data Sheets*, **113**(n/a), 2187–389. DOI: 10.1016/j.nds.2012.10.001
- Basu, S.K. and McCutchan, E.A. (2020). Nuclear data sheets for A=90. *Nuclear Data Sheets*, **165**(n/a), 1–329. DOI: 10.1016/j.nds.2020.04.001
- Brown, B.A. (2005). *Lecture Notes in Nuclear Structure Physics National Super Conducting Cyclotron Laboratory and Department of Physics and Astronomy*. Michigan state university, USA: E Lansing, MI, 48824, 290.
- Brown, B.A. and Rae, W.D.M. (2014). The shell model code nushellx@msu. *Nuclear Data Sheets*, **120**(n/a), 115–8. DOI: 10.1016/j.nds.2014.07.022.

Carchidi, M., Wildenthal, B.H. and Brown, B.A. (1986). Quadrupole

moments of sd-shell nuclei. *Physical Review C*, **34**(6), 2280–97. DOI: 10.1103/PhysRevC.34.2280

- Hasan, A.K., Obeed, F.H. and Rahim, A.N. (2021). Study of the electric quadrupole transitions in 50-51 Mn isotopes by using f742pn and f7cdpn interactions. *The Scientific Journal of King Faisal University: Basic and Applied Sciences*, **22**(2), 11–5. DOI: 10.37575/b/sci/0070
- Heng, W.Y., Yang, D., Yan, M.K. and Wei, L.P. (2019). Investigation of the level structure of 90Nb nucleus using the shell-model. *Nukleonika*, **64**(4), 113–6. DOI: 10.2478/nuka-2019-0014
- Heyde, K.L.G. and Irvine, J.M. (1990). *The Nuclear Shell-model*. Berlin, Heidelberg, Germany: Springer.
- Lawson, R.D. (1980). *Theory of the Nuclear Shell-model*. Oxford, United Kingdom: Clarendon Press.
- Negretand, A. and Sonzogni, A.A. (2011). Adopted levels, gammas for 94sr isotope. *Nuclear Data Sheets*, **6**(n/a), n/a.
- Obeed, F.H. (2021). Calculation of nuclear properties for 56–62Fe isotopes in the model space ho. *Ukrainian Journal of Physics*, **66**(8), 643–52. DOI: 10.15407/ujpe66.8.643
- Obeed, F.H. and Hasan, A.K. (2021). Calculation of quadrupole deformation parameter (β_2) from reduced transition probability $B(E2)^\uparrow$ for transition ($0_1^+ \rightarrow 2_1^+$) at even-even 62-68zn isotopes. *Nuclear Physics and Atomic Energy*, **1**(22), 30–41. DOI: 10.15407/jnpae2021.01.030
- Pattabiraman, N. S., Chintalapudi, S. N., Ghugre, S. S., Rao, B. T., Raju, M. L. N., Reddy, T. S. and Jain, H. C. (2002). Level structure of 92 Mo at high angular momentum: Evidence for Z= 38, N= 50 core excitation. *Physical Review C*, **65**(4), 044324. DOI:10.1103/PhysRevC.65.044324
- Preetha, P. and Kumar, S.S. (2017). Reduced transition probability B(E2) in even-even Ti isotopes. In: *62nd DAE-BRNS Symposium on Nuclear Physics*. Thapar University, Patiala, India, 20–24 /12/2017.
- Rainovski, G., Schwengner, R., Schilling, K. D., Wagner, A., Jungclaus, A., Galindo, E. and Kröll, T. (2002). High-spin structure of the spherical nucleus 90 Y. *Physical Review C*, **65**(4), 044327. DOI: 10.1103/PhysRevC.65.044327.
- Roy, R. and Nigam, B. (1967). *Nuclear Physics. Theory and Experiment*. Hoboken, Jersey, New York: John Wiley and Sons Inc.
- Salman, A.D. and Hameed, S.M. (2022). Study the nuclear structure of 6Li nuclei with the calculation of a large basis shell-model. In: *AIP Conference Proceedings, 3rd International Scientific Conference of Alkafeel University*. Alkafeel University, Najaf, Iraq, 22–23/3/2021.